11th World Congress on Computational Mechanics (WCCM XI)
5th European Conference on Computational Mechanics (ECCM V)
6th European Conference on Computational Fluid Dynamics (ECFD VI)
E. Oñate, J. Oliver and A. Huerta (Eds)

MYOCARDIAL TISSUE MECHANICS WITH FIBRES MODELLED AS ONE-DIMENSIONAL COSSERAT CONTINUA

S. Skatulla*, K. Sack* and C. Sansour†

* CERECAM, Dept. of Civil Engineering,
University of Cape Town, South Africa,
email: sebastian.skatulla@uct.ac.za, http://www.skatulla.com

† Division of Materials, Mechanics, and Structures,
The University of Nottingham, United Kingdom,
carlo.sansour@nottingham.ac.uk, http://www.nottingham.ac.uk

Key words: Soft tissue mechanics, Cardiac mechanics, Cosserat Continua

Abstract. Classically, the elastic behaviour of cardiac tissue mechanics is modelled using anisotropic strain energy functions capturing the averaged behaviour of its fibrous microstructure. The strain energy function can be derived via representation theorems for anisotropic functions where a suitable nonlinear strain tensor, e.g. the *Green* strain tensor, describes locally the current state of strain. These kinds of approaches, however, are usually of phenomenological nature and do not elucidate on the complex heterogeneous material composition of cardiac tissue characterized by different fibre hierarchies interwoven by collagen, elastin and coronary capillaries. Thus, pathological changes of microstructural constituents, e.g. with regards to the extra-cellular matrix, and their implications on the macroscopically observable material behaviour cannot be directly investigated.

This paper follows a hypothesis by Hussan et al. [24], stipulating that the semisoft behaviour of myocardial tissue stems from the ability of cardiac myocytes to deform while being embedded and constrained by the cross-linked collagen matrix. Here, the fibrous characteristics of the myocardium are modelled by one-dimensional *Cosserat* continua. This additionally allows for the inclusion of fibre motion relative to matrix representing the non-local material response due to twisting and bending of fibres.

1 INTRODUCTION

Cardiovascular disease is the single leading cause of death in the world accounting for 30% of all human mortality [2]. Despite the recent advancements of pharmaceutical,

surgical, device and tissue engineered therapy strategies, cardiovascular disease remains one of the most costly, common and deadly medical conditions. Despite current worldwide efforts to treat cardiovascular disease, projections show an increase in predicted mortality[1], keeping cardiovascular disease as the leading cause of death globally [28, 2]. Historically, clinical treatments for cardiovascular disease have been developed primarily by trial and error as opposed to a comprehensive understanding of the structural and mechanical changes that a diseased heart undergoes. Recent advancements in numerical methods and the proliferation of inexpensive high performance computing power has enabled more sophisticated simulation tools that could allow for greater insight into cardiovascular disease and guide the development of modern therapies.

Cardiovascular tissue is a complex heterogeneous material with a significant hierarchical micro structure that influences the material on a macro scale. [17, 33, 22, 36]. Mathematically this is classified as a non-linear, hyperelastic material with orthotropic properties arising from the micro-structure influence of the myocyte fibres.

The need to place a larger emphasis on the micro structure is expressed heavily in the literature [38, 21, 18]. Specifically over the last 15 years, models have introduced phenomenological properties as a means to overcome the complex structure on a macro and micro scale. Increasing attempts to include the micro structural influences have emerged with the hope to better capture the complex material response by placing a larger influence on the multi-scale physics underlying the behaviour. [37] introduced a one of the first multi-scale models, by including cellular considerations for calculating the global active tension during contraction. [24] includes micro mechanical contributions from the myocytes (and their perimysial collagen mesh), modelling them as cylinders with mechanical degrees of freedom corresponding to twist, bend and splay. In the mechanical modelling of hard biological tissue, various micro continuum approaches have also been investigated [40, 30, 1, 9]. However soft biological tissue remains to be significantly under investigated with respect to micro continuum theories.

This research intends to adopt the work of []Sansour2008 and extend its application to soft biological tissue. The fibrous cardiac tissue will be mathematically represented through the inclusion of one dimensional *Cosserat* rods in the formulation of the material's kinematics and constitutive laws. The successful inclusion of generalized continua approaches, including *Cosserat* models, in the application to other hard biological tissue, i.e bone [30, 1, 17, 33], has proved successful in capturing more realistic material responses.

Investigation into the higher order contributions from the one dimensional rods will be analysed in application to small cardiac specimens and left ventricular representations.

[1]Reliable projections up until 2030.

2 METHOD

We decompose the strain energy in contributions related to fibrous structural components, e.g. bundles of myocytes embedded in perimysial collagen, modelled by one-dimensional *Cosserat* continua and complementary connective tissue. In the *Cosserat* continuum every material point P is assigned besides displacement additional rotational degrees of freedom described by a rotation tensor $\mathbf{R} \in SO(3)$ which is independent of the deformation gradient $\mathbf{F}$. This allows for the formulation of two strain measures, a stretch-like strain tensor $\mathbf{U} = \mathbf{R}^T\mathbf{F}$ and a change of curvature strain tensor $\mathbf{K} = -\frac{1}{2}\boldsymbol{\epsilon} : (\mathbf{R}^T\mathbf{R}_{,i}) \otimes \mathbf{V}_i$ where the index $i = f, t, n$ and $\mathbf{V}_f, \mathbf{V}_t, \mathbf{V}_n$ span an orthonormal basis describing fibre, sheet-tangent and sheet-normal directions, respectively.
A *Fung*-type orthotropic strain energy function $\psi(\mathbf{U}, \mathbf{K})$ incorporating fibrous and complementary matrix material components is defined as follows:

$$\psi = \frac{1}{2} A \left(\exp^{BQ} - 1\right) + A_{comp} \left(J \ln J - J + 1\right) \tag{1}$$

with J denoting the Jacobian and the exponent $Q = Q_{fibre} + Q_{matrix}$ given by

$$Q_{fibre} = a_1 U_{ff}^2 + a_2 \left(U_{ff}^2 + U_{tf}^2 + U_{nf}^2\right) + \sum_i^N \left\{ a_3^{(i)} K_{ff}^2 + a_4^{(i)} \left(K_{ff}^2 + K_{tf}^2 + K_{nf}^2\right) \right\} \tag{2}$$

$$Q_{matrix} = b_1 \left(U_{tt}^2 + U_{nn}^2\right) + b_2 \left(U_{ft}^2 + U_{tt}^2 + U_{nt}^2 + U_{fn}^2 + U_{tn}^2 + U_{nn}^2\right) \tag{3}$$

considering the heterogeneous responses of N different hierarchical fibre entities and the associated material parameters A, B, A_{comp}, a_1, a_2, $a_3^{(i)}$, $a_4^{(i)}$, b_1 and b_2.
Finally, a corresponding variational principle is formulated as

$$\int_{\mathcal{B}} \left\{ \boldsymbol{n} : \delta\mathbf{U} + \boldsymbol{m} : \delta\mathbf{K} \right\} \mathrm{d}V - W_{ext} = 0 \tag{4}$$

with the force stress tensor $\boldsymbol{n} = \dfrac{\partial\psi}{\partial\mathbf{U}}$ and the couple stress tensor $\boldsymbol{m} = \dfrac{\partial\psi}{\partial\mathbf{K}}$. The latter incorporates the heterogeneous responses of all considered fibrous constituents.

3 RESULTS

Calibration

Considering in Eq. (3) only one fibrous constituent, i.e. bundles of myocytes interwoven by perimysial collagen, and assuming equal elasticity moduli for first and higher-order strains, respectively, i.e. $a_3 = a_2$, $a_4 = a_1$, then the proposed transverse isotropic tissue model in Eq. (1) has four material anisotropy parameters a_1, a_2, b_1 and b_2; two stress scaling parameters A and A_{comp}, relating to compressible and incompressible contributions, respectively; an exponential scaling parameter B; and the characteristic length l which is a feature of the micro structure.

The availability of experimental data suitable for the calibration of cardiac tissue is limited. The most comprehensive study investigating orthotropy was performed by [13] in which cubic sections cut from a porcine left ventricle were subject to shear loads. The experiment was performed to include all six combinations of fibre orientation and shear deformation as illustrated in Figure 1. In case of other animals, one can utilize a common assumption that one mammalian specific cardiac material behaves in a similar manner to other mammalian cardiac tissue [14]. Based on this assumption, the material anisotropy parameters (l, a_1, a_2, b_1 and b_2) are directly calibrated using the shear experiments. To complete the material parameter calibration, a secondary calibration is employed to obtain the remaining "scaling" parameters to fit animal specific models using experimental data, e.g. ventricular pressure-volume curves or cavity surface deformation data, pertaining directly to the animal in question. In this sense the scaling parameters A and B are considered specific material parameters for a given species. The other material parameters l, a_1, a_2, b_1 and b_2 are considered universal cardiac tissue parameters that govern the anisotropy and include a feature of the micro structure, these remain unchanged from species to species.

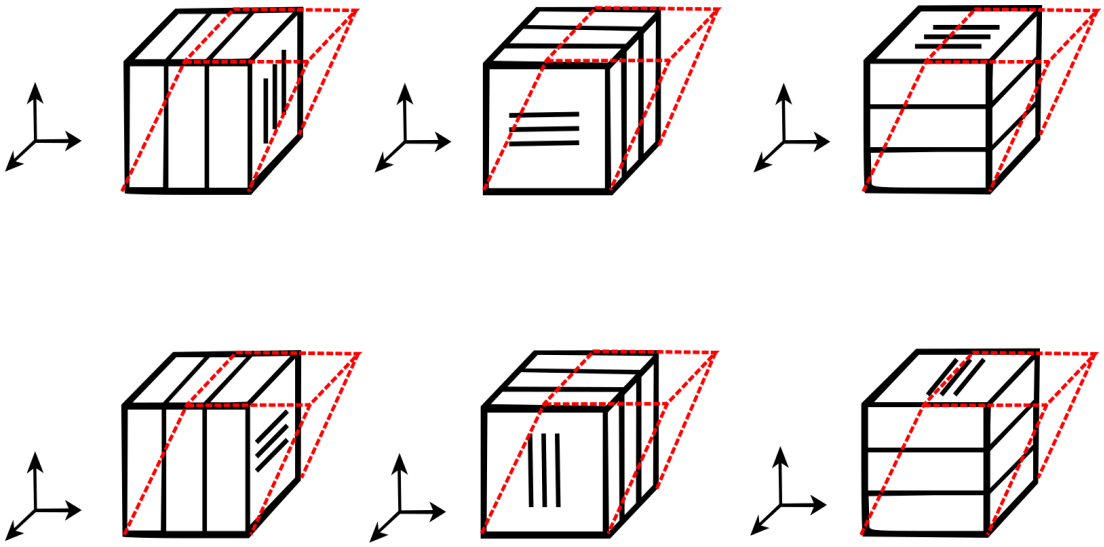

Figure 1: Sketches of six possible modes of shear for orthotropic myocardium defined with respect to the fibre axis f, sheet-tangent axis t and sheet-normal axis n.

For the special case of calibrating transverse isotropy, we recognise that the total combinations of fibre orientation and shear deformation reduces to three possible cases as put forward in Figure 2.

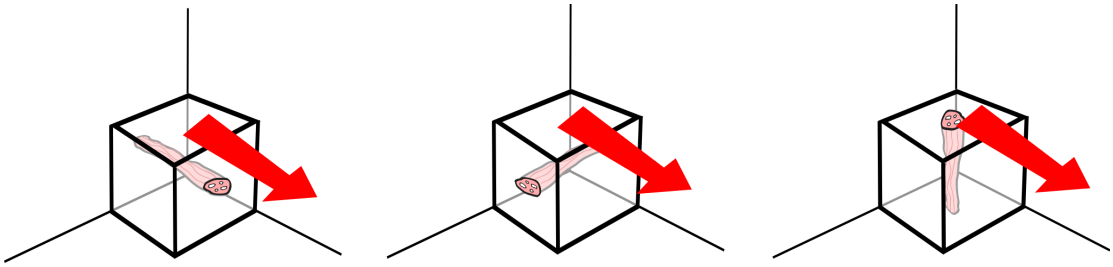

Figure 2: Sketches of the three possible modes of shear for transverse isotropic myocardium: (a) A transverse plane shifted towards the fibre direction, (b) a transverse plane shifted towards the other transverse plane and lastly (c) the fibre plane shifted towards a transverse plane.

The specimen cubes used in the shear experiments of [13], had a natural variation in the fibre orientation. The cube dimensions were $3mm \times 3mm \times 3mm$, extracted from the midwall of the left ventricle and rejected if there was a change in fibre orientation amounting to more than 30° across the cube. In order to represent this in our shear experiments, and following the work of [24], we specify a mean fibre orientation in our cube and allow for that orientation to vary. The variation of the fibre orientation is considered a smooth function of one transverse direction. This results in the fibre direction on one side of the cube orientated $+15^{\circ}$ from the mean direction and -15° on the opposite side.

The varying fibre orientation is a necessary requirement in order to calibrate for the characteristic length l, as it introduces torsional and flexural strain in the deformation of the cube.

In order to calibrate the transverse isotropic case we are forced to combine the original data sets into the relevant three cases outlined in Figure 2. The combined data sets were constructed by fitting an exponential function to pairs of data using MATLAB's built in curve fitting algorithm. The data sets were equally weighted using the least root mean square fit produced the resulting "midline" data set.

The computational reproduction of the experiments are designed to reproduce the experimental design in [13] as accurately as possible. Using the same specified dimensions ($3mm \times 3mm \times 3mm$) each cube is fixed at the bottom with respect to all displacements, while the top surface experiences shear displacements amounting to 50% of the cube's length. The top and bottom surface were glued to plates, in the shearing device used by Dokos, and as such while shearing the top surface, the displacements in the remaining directions remain fixed. Additionally, we impose appropriate rotational boundary conditions on the top and bottom surface, resulting in all rotations being constrained along the top and bottom surface.

Research done in the Computational Continuum Mechanics Group, UCT, established

an optimization scheme based on the Bounded Levenberg-Marquardt algorithm or BLVM [27]. For a detailed account of the optimization and corresponding implementation one is directed to [15]. Material parameter identification is found via minimization of a cost function, expressing the difference between experimental data points and corresponding simulation results. Initial material parameters choices need to specified, including constraints on the reasonable parameter choices. For the calibration of the nonlinear *Cosserat* fibre model, the optimization algorithm was applied separately to the three cases outlined in Figure 2. This forced the authors to perform multiple rounds of calibration to identify suitable parameters. After the first iteration of calibration, any consistent results across the three experiments was taken as a successfully calibrated parameters and was fixed, or tightly constrained, for the successive rounds of calibration. All parameters were subject to calibration through the optimization routine, except for B and A_{comp} which were both set to 1.00. It would be redundant to calibrate for B in such a problem and simple shear is volume preserving and as such A_{comp} plays no role. l is calibrated to achieve the lowest possible residual in the optimization routine.

Calibration results

The *Cosserat* fibre model is able to reproduce the experimental results for porcine myocardium relatively well. The resulting fitted model, plotted alongside the data sets used are shown in Figure 3. The fitted parameters are presented in the Table 1.

Table 1: Material properties for nonlinear *Cosserat* constitutive law, fitted to [13] shear experimental data for porcine cardiac tissue.

Parameter	Symbol	Value
Principle fibre modulus	a_1	52.380
Shear fibre modulus	a_2	28.090
Principle matrix modulus	b_1	18.112
Shear matrix modulus	b_2	16.480
Characteristic length	l	0.6622
Stress Scaling 1	A	0.10
Stress Scaling 2	B	1.00
Incompressibility	A_{comp}	1.00

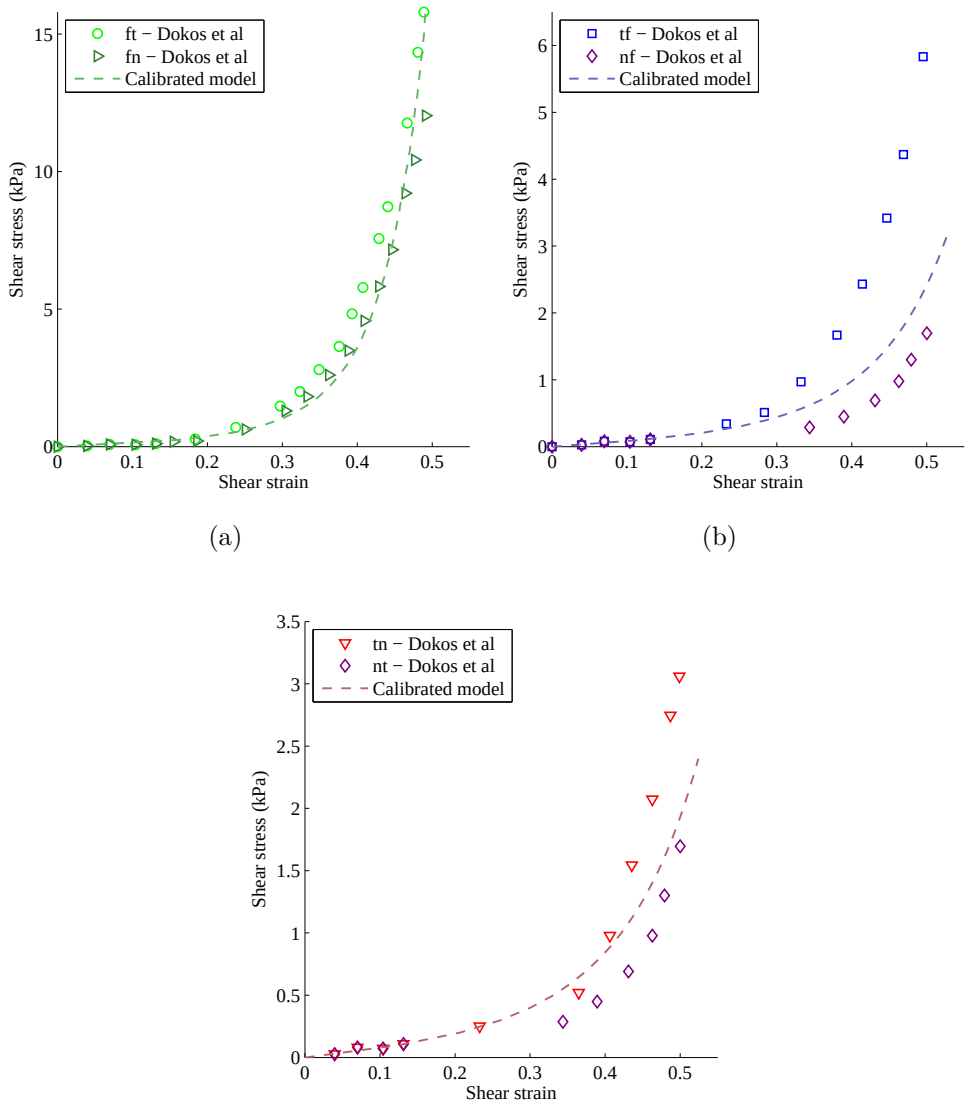

Figure 3: Material response of calibrated nonlinear *Cosserat* fibre model (dashed lines) alongside the combined data sets from [13]. (a) The fibre plane shifted towards a transverse plane, (b) a transverse plane shifted towards the fibre direction and lastly, (c) a transverse plane shifted towards the other transverse plane.

In Figure 4, the calibrated *Cosserat* fibre model result is presented alongside the case where higher order strains are excluded (i.e $l = 0.0$) for the shear experiment of a cube extending the plane normal to the fibre in the transverse direction. The case where $l = 0.0$ includes only first order strains in its constitutive description and as such is more

compliant. One could recalibrate the model to coincide more closely with the experimental data, but in this sense one would be placing a larger dependence on local features, i.e that the stress at the material point is solely governed by first order strains. The *Cosserat* fibre continuum theory, accounts for the influence of relative motion of neighbouring material points resulting in torsional and flexural strains, i.e. introducing higher-order strains. These are the change of curvature strains along the fibre. These contributions, scaled by l, provide a direct and meaningful way of including the underlying micro-structural kinematics and more accurately representing the material.

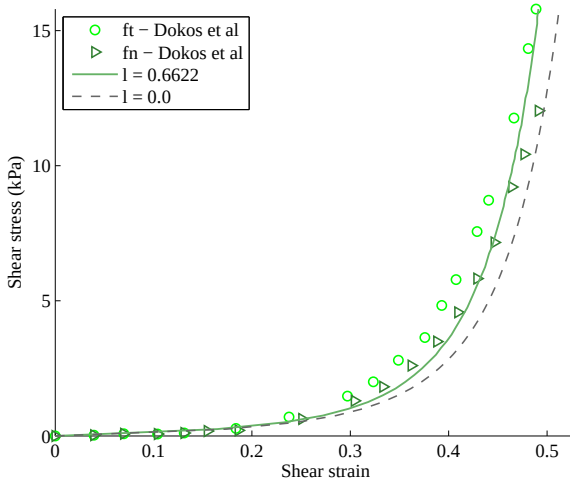

Figure 4: Material response of calibrated nonlinear *Cosserat* fibre model alongside the classical case for the same material parameters.

4 CONCLUSIONS

In summary, the proposed approach is motivated by the microstructural kinematics of myocytes and bundles of myocytes interacting with the collagen enmeshment. It describes the passive material behaviour of cardiac tissue through the *Cosserat* fibre continuum. The defining feature of the model, the characteristic length l, controls the influence of higher-order strains arising from relative motion of the micro-structural constituents. Consequently, pathological changes of the latter and their impact on micro-mechanical properties can be specifically addressed in a more detailed fashion.

It is demonstrated that the proposed nonlinear transversely isotropic constitutive law based on the *Cosserat* fibre continuum is able to closely reproduce the shear experimental data of [13]. In particular, the influence of fibre orientation and variation across the tissue specimen gives rise to higher-order micro-structural deformation such as twist and flexure which can be directly accounted for by the change of curvature strains which are a key feature of the *Cosserat* continuum.

5 ACKNOWLEDGEMENT

The research leading to this work has been supported by the Centre for High Performance Computing of South Africa.

REFERENCES

[1] EC Aifantis. Strain gradient interpretation of size effects. *International Journal of Fracture*, 95(1-4):299–314, 1999.

[2] Ala Alwan et al. *Global status report on noncommunicable diseases 2010.* World Health Organization, 2011.

[3] Arnaud Bistoquet, John Oshinski, and Oskar Skrinjar. Left ventricular deformation recovery from CINE MRI using an incompressible model. *Medical Imaging, IEEE Transactions on*, 26(9):1136–1153, 2007.

[4] L. K. Waldman, Y. C. Fung, and J. W. Covell. Transmural myocardial deformation in the canine left ventricle. normal in vivo three-dimensional finite strains. *Circ Res*, 57(1):152–63, Jul 1985.

[5] Hiroshi Ashikaga, Benjamin A Coppola, Katrina G Yamazaki, Francisco J Villarreal, Jeffrey H Omens, and James W Covell. Changes in regional myocardial volume during the cardiac cycle: implications for transmural blood flow and cardiac structure. *American Journal of Physiology-Heart and Circulatory Physiology*, 295 (2):H610–H618, 2008.

[6] Ignacio Rodriguez, Daniel B Ennis, and Han Wen. Noninvasive measurement of myocardial tissue volume change during systolic contraction and diastolic relaxation in the canine left ventricle. *Magnetic resonance in medicine*, 55(3):484–490, 2006.

[7] Cory Swingen, Xiaoen Wang, and Michael Jerosch-Herold. Evaluation of myocardial volume heterogeneity during end-diastole and end-systole using cine mri. *Journal of Cardiovascular Magnetic Resonance*, 6(4):829–835, 2004.

[8] Maurice B Buchalter, James L Weiss, Walter J Rogers, Elias A Zerhouni, Myron L Weisfeldt, Rafael Beyar, and Edward P Shapiro. Noninvasive quantification of left ventricular rotational deformation in normal humans using magnetic resonance imaging myocardial tagging. *Circulation*, 81(4):1236–1244, 1990.

[9] PM Buechner and RS Lakes. Size effects in the elasticity and viscoelasticity of bone. *Biomechanics and Modeling in Mechanobiology*, 1(4):295–301, 2003.

[10] Oscar H Cingolani, Xiao-Ping Yang, Maria A Cavasin, and Oscar A Carretero. Increased systolic performance with diastolic dysfunction in adult spontaneously hypertensive rats. *Hypertension*, 41(2):249–254, 2003.

[11] Kim A Connelly, David L Prior, Darren J Kelly, Michael P Feneley, Henry Krum, and Richard E Gilbert. Load-sensitive measures may overestimate global systolic function

in the presence of left ventricular hypertrophy: a comparison with load-insensitive measures. *American Journal of Physiology-Heart and Circulatory Physiology*, 290(4): H1699–H1705, 2006.

[12] K. D. Costa, J. W. Holmes, and A. D. McCulloch. Modelling cardiac mechanical properties in three dimensions. *Philosophical Transactions of the Royal Society A*, 359:1233–1250, 2001.

[13] Socrates Dokos, Bruce H. Smaill, Alistair A. Young, and Ian J. LeGrice. Shear properties of passive ventricular myocardium. *American Journal of Physiology - Heart and Circulatory Physiology*, 283:H2650–H2659, 2002.

[14] Matthew G. Doyle, Stavros Tavoularis, and Yves Bourgault. Adaptation of a rabbit myocardium material model for use in a canine left ventricle simulation study. *Journal of Biomechanical Engineering*, 132(4):041006, 2010.

[15] M. A. Essack and S. Skatulla. Matthew G. Doyle, Stavros Tavoularis, and Yves Bourgault. Material Parameter Identification for Modelling the Left Ventricle in the Healthy State *Computers & Structures*, 2014. under review.

[16] G M Faber and Y Rudy. Action potential and contractility changes in [na+](i) overloaded cardiac myocytes: A simulation study. *Biophysical Journal*, 78:2392–2404, 2000.

[17] J Fatemi, F Van Keulen, and PR Onck. Generalized continuum theories: Application to stress analysis in bone*. *Meccanica*, 37(4-5):385–396, 2002.

[18] S. Göktepe, S. N. S. Acharya, J. Wong, and E. Kuhl. Computational modeling of passive myocardium. *International Journal for Numerical Methods in Biomedical Engineering*, 27(1):1–12, 2011. ISSN 2040-7947.

[19] J. M. Guccione, K. D. Costa, and A. D. McCulloch. Finite element stress analysis of left ventricular mechanics in the beating dog heart. *Journal of Biomechanical Engineering*, 28:1167–1177, 1995.

[20] Keith L Herrmann, Andrew D McCulloch, and Jeffrey H Omens. Glycated collagen cross-linking alters cardiac mechanics in volume-overload hypertrophy. *American Journal of Physiology-Heart and Circulatory Physiology*, 284(4):H1277–H1284, 2003.

[21] G. A. Holzapfel and R. W. Ogden. Constitutive modelling of passive myocardium: a structurally based framework for material characterization. *Philosophical Transactions of the Royal Society a-Mathematical Physical and Engineering Sciences*, 367 (1902):3445–3475, Sep 13 2009. ISSN 1364-503X.

[22] Gerhard A Holzapfel, Thomas C Gasser, and Ray W Ogden. A new constitutive framework for arterial wall mechanics and a comparative study of material models. *Journal of elasticity and the physical science of solids*, 61(1-3):1–48, 2000.

[23] J.D. Humphrey and FC Yin. Constitutive relations and finite deformations of passive cardiac tissue ii: stress analysis in the left ventricle. *Circulation research*, 65(3):805–817, 1989.

[24] Jagir R Hussan, Mark L Trew, and Peter J Hunter. A mean-field model of ventricular muscle tissue. *Journal of biomechanical engineering*, 134(7), 2012.

[25] David Jegger, Ajit S Mallik, Mohammed Nasratullah, Xavier Jeanrenaud, Rafaela da Silva, Hendrik Tevaearai, Ludwig K von Segesser, and Nikolaos Stergiopulos. The effect of a myocardial infarction on the normalized time-varying elastance curve. *Journal of Applied Physiology*, 102(3):1123–1129, 2007.

[26] Roy Kerckhoffs. *Depolarization wave and mechanics in the paced heart: model and experiment*. PhD thesis, Tehcnical University of Eindhoven, 2003.

[27] Kenneth Levenberg. A method for the solution of certain problems in least squares. *Quarterly of applied mathematics*, 2:164–168, 1944.

[28] C Mathers and Dejan Loncar. Updated projections of global mortality and burden of disease, 2002-2030: data sources, methods and results. *Geneva: World Health Organization*, 2005.

[29] Jeffrey H Omens, Deidre A MacKenna, and Andrew D McCulloch. Measurement of strain and analysis of stress in resting rat left ventricular myocardium. *Journal of biomechanics*, 26(6):665–676, 1993.

[30] HC Park and RS Lakes. Cosserat micromechanics of human bone: strain redistribution by a hydration sensitive constituent. *Journal of biomechanics*, 19(5):385–397, 1986.

[31] Frank E Rademakers, MB Buchalter, Walter J Rogers, Elias A Zerhouni, Myron L Weisfeldt, James L Weiss, and Edward P Shapiro. Dissociation between left ventricular untwisting and filling. accentuation by catecholamines. *Circulation*, 85(4): 1572–1581, 1992.

[32] Espen W Remme, Alistair A Young, Kevin F Augenstein, Brett Cowan, and Peter J Hunter. Extraction and quantification of left ventricular deformation modes. *Biomedical Engineering, IEEE Transactions on*, 51(11):1923–1931, 2004.

[33] Josef Rosenberg and Robert Cimrman. Microcontinuum approach in biomechanical modeling. *Mathematics and Computers in Simulation*, 61(3):249–260, 2003.

[34] C. Sansour and S. Skatulla. A non-linear Cosserat continuum-based formulation and moving least square approximations in computations of size-scale effects in elasticity. *Computational Materials Science*, 41:589–601, 2008.

[35] Thomas F Schaible, Ashwani Malhotra, Gary Ciambrone, and James Scheuer. The effects of gonadectomy on left ventricular function and cardiac contractile proteins in male and female rats. *Circulation research*, 54(1):38–49, 1984.

[36] A. Schmidt, C.F. Azevedo, A. Cheng, S.N. Gupta, D.A. Bluemke, T.K. Foo, G. Gerstenblith, R.G. Weiss, E. Marban, G.F. Tomaselli, et al. Infarct tissue heterogeneity by magnetic resonance imaging identifies enhanced cardiac arrhythmia susceptibility in patients with left ventricular dysfunction. *Circulation*, 115(15):2006, 2007.

[37] NP Smith, DP Nickerson, EJ Crampin, and PJ Hunter. Multiscale computational modelling of the heart. *Acta Numerica*, 13(1):371–431, 2004.

[38] James Southern, Joe Pitt-Francis, Jonathan Whiteley, Daniel Stokeley, Hiromichi Kobashi, Ross Nobes, Yoshimasa Kadooka, and David Gavaghan. Multi-scale computational modelling in biology and physiology. *Progress in Biophysics and Molecular Biology*, 96(1-3):60 – 89, 2008. ISSN 0079-6107. Cardiovascular Physiome.

[39] Kazunori Uemura, Toru Kawada, Masaru Sugimachi, Can Zheng, Koji Kashihara, Takayuki Sato, and Kenji Sunagawa. A self-calibrating telemetry system for measurement of ventricular pressure-volume relations in conscious, freely moving rats. *American Journal of Physiology-Heart and Circulatory Physiology*, 287(6):H2906–H2913, 2004.

[40] JFC Yang and Roderic S Lakes. Experimental study of micropolar and couple stress elasticity in compact bone in bending. *Journal of biomechanics*, 15(2):91–98, 1982.